ISSN 0005-1144
ATKAFF 50(3–4), 234–244(2009)

Zvonimir Šipuš, Marko Bosiljevac, Ivan Lujo

Specialty Optical Fibers: Analysis and Characterization

UDK 681.7.068
IFAC 4.3.2

Original scientific paper

This paper gives a closer insight to novel optical fibers by applying specialized numerical analysis approaches. First we have described a newly developed algorithm based on the spectral domain approach, which is employed in the analysis of multilayer optical fibers with circular symmetry. It computes the Green's functions of the considered fiber and locates the appropriate poles, which correspond to the actual propagating modes of the fiber. Through further analysis of the poles it is possible to obtain information about modal fields, attenuation, bending losses and dispersion properties for all modes present in fibers with very complicated refractive index profile. Furthermore, an approach for the analysis of novel types of fibers belonging to the so-called Photonic Crystal Fibers family is presented. Since the considered fibers can contain various inclusions in the core or the cladding structure, the analysis is in this case based on the modal decomposition of the electric field in spatial domain. In both analysis cases the obtained results were compared to the previously published or where possible measured results, showing very good agreement.

Key words: Optical fibers, Multilayer fibers, Spectral domain analysis, Holey fibers, Dispersion, Optical losses

Specijalna optička vlakna: analiza i karakterizacija. U ovom radu, primjenom specijaliziranih numeričkih postupaka, dan je detaljan uvid u nove vrste optičkih vlakna. U prvom dijelu opisan je algoritam za analizu kružnosimetričnih višeslojnih optičkih vlakana, koji se temelji na spektralnom pristupu. Algoritam izračunava Greenove funkcije promatranih vlakana, te locira polove koji odgovaraju propagirajućim modovima u samom vlaknu. Daljnjom analizom svojstava polova moguće je za sve prisutne modove dobiti vrijednosti polja u svjetlovodu, parametre gušenja, gubitke uslijed savijanja i disperzijska svojstva. Pri tome samo optičko vlakno može imati vrlo složen profil indeksa loma. U drugom dijelu prikazan je pristup za analizu novih vrsta svjetlovoda koji spadaju u grupu tzv. fotoničkih kristalnih svjetlovoda. Ovi svjetlovodi mogu sadržavati razne varijacije u strukturi jezgre ili plašta, te je stoga analiza u ovom slučaju temeljena na modalnoj dekompoziciji električnog polja u prostornoj domeni. U oba razmatrana slučaja dobiveni rezultati se dobro poklapaju s ranije objavljenim rezultatima, ili gdje je to bilo moguće, s mjernim rezultatima.

Ključne riječi: optička vlakna, višeslojni svjetlovodi, spektralna metoda analize, svjetlovodi sa zračnim kapilarama, disperzija, optički gubici

1 INTRODUCTION

Optical fibers are the foundation stone of all modern global telecommunication systems. Their application begun in the early seventies in the last century with the first fibers with low attenuation (< 20 dB/km) and through continuous research and development they became irreplacable in todays information society. However, in the recent years standard optical fibers have almost reached the physical limitations of the medium they use (silica glass - SiO_2). This is quite understandable if we take into account that the basic principles of guiding systems haven't changed since the 19th century. In other words, all the key elements of the optical fiber technology were defined very early (25 years ago) and all subsequent development was just incremental improvement of specific components. Today's modern fibers are therefore a compromise between optical losses, dispersion, nonlinear and polarization effects. Some of these effects are connected only with the properties of the materials used (e.g. losses), while others can be avoided by proper design of the fibers (e.g. dispersion). Nevertheless, mentioned compromises represent practically the peak of the used technology and for further development it is necessary to start thinking differently.

In the last ten years, significant progress has been made with new types of optical fibers: Photonic Crystal Fibers (PCF), bend loss free fibers, dispersion-compensating fibers, etc [1]. Essential idea behind most of these fibers is the application of some alternative type of cladding (needed for obtaining total reflection property), which in most cases means the use of periodical structures as or a

part of the cladding. The advantage of having a periodical structure as cladding lies in the possibility to manipulate the basic guiding properties of the fiber. As a consequence it is possible to develop fibers that can have a core with a refractive index lower then the one of the cladding and even air can be used in which case we get a so-called hollow fiber. Different approach is to use periodicity only in a part of the cladding. This can be done for example by introducing periodical holes in the structure of the cladding. The holes effectively reduce the refractive index of the cladding and therefore there is no need for a different cladding material and the result can be a fiber made completely out of silica.

Possible applications of this fibers span from high power transmission to very low bend loss fibers (application which is particularly interesting for Fiber To The Home (FTTH) networks because it is hard to avoid fiber bending when installing fibers inside the buildings). Dispersion and polarization properties can be custom tailored to meet specific requirements, fibers can be designed to be single mode for a very wide range of wavelengths (endless single mode fibers), and also various new fiber lasers and fiber sensors can now be realized.

All of these new ideas however require new analysis tools, which can deal with various fiber structures, different layers and geometries. This is a very difficult task and it is very hard to efficiently analyze a wide range of structures. General purpose EM solvers based on Finite Element Method (FEM) or Finite Difference Time Domain (FDTD) usually need very large computational time and consume large computer resources. Because of that specific analysis tools are being developed which by adapting to some specific geometry or structure can be very efficient and accurate in the prediction of various fiber parameters such as attenuation, chromatic and polarization dispersion, bending losses and non-linear effects.

The analysis approach based on spectral domain method which can be very efficiently used for characterization of fibers with multilayered claddings is presented in the first part (Section 2.1) of this paper. These special fibers are used for dispersion compensation applications, as low bend loss fibers and even for newly developed in-fiber high power lasers. The following section (Section 2.2) will present the results for different geometries of the fibers and give a better insight into the application possibilities. The second part (Section 3) of the paper is dedicated to the analysis and measurements of so-called holey fibers which are a representative of the continuously growing PCF family of fibers.

2 FIBERS WITH MULTILAYERED CLADDING

2.1 Analysis

The modes in standard optical fibers are usually determined by the following procedure: first the *E* and *H*-field components are written in terms of Bessel and Hankel functions, then the system of linear equations is set by fulfilling the boundary conditions for tangential *E*- and *H*-field components at the layer boundaries, and finally the modes are determined by solving the system of linear equations. Such an approach of analyzing step-index fibers with the one-layer core can be found in many text books (see e.g. [2]). The graded-index fiber can also be analyzed in this way by using a stepwise approximation of refractive index [3]. In the case of multilayer fibers such a procedure is very cumbersome, and therefore there is a need for a numerical routine that can treat general multilayer optical fibers. For this purpose we use the numerical algorithm, called G1DMULT, for determining the Green's function of circular-cylindrical multilayered fiber structure. From the properties of Green's functions we can then determine all the effects of wave propagation inside the fiber. The advantage of this approach is that optical fibers with arbitrary number of layers can be analyzed, and it is easy to modify the program in order to analyze more complex problems (for example, cases where physical or equivalent sources are included).

The G1DMULT algorithm is based on the spectral domain approach where a three-dimensional problem is transformed into a spectrum of one-dimensional problems by performing a two-dimensional Fourier transformation in the coordinates for which the structure is homogeneous. In the circular-cylindrical case, we perform the Fourier transformation in the axial direction and the Fourier series in the ϕ direction [4]:

$$\tilde{\mathbf{E}}(\rho, m, k_z) = \int_{-\infty}^{\infty} \int_{0}^{2\pi} \mathbf{E}(\rho, \phi, z) e^{jm\phi} e^{jk_z z} d\phi dz. \quad (1)$$

By doing so, for each spectral component of the source, the excited electromagnetic field in the two directions for which the structure is homogeneous has the same harmonic variation as the source. As a result, only the electromagnetic field variation in the direction normal to the surface is unknown. This allows for the rigorous analysis of complex multilayered structures, if the layers are homogeneous as described. Of course, to determine the actual fields one needs to return to the spatial domain by performing the inverse Fourier transformation. For our circular cylindrical case it would mean one-dimensional inverse Fourier transformation in the *z* direction and the inverse Fourier series

in the ϕ direction

$$\mathbf{E}(\rho,\phi,z)=\frac{1}{4\pi^2}\sum_{m=-\infty}^{\infty}\int_{-\infty}^{\infty}\tilde{\mathbf{E}}(\rho,m,k_z)e^{-jm\phi}e^{-jk_z z}dk_z. \tag{2}$$

The structure of the G1DMULT algorithm is the following one. First step inside the algorithm is to make a division of the original electromagnetic problem into a set of equivalent sub-problems [5], see Fig. 1(a) and 1(b). The unknowns inside each equivalent sub-problem are the tangential *E*- and *H*- fields at the layer boundaries (Fig. 1(c)). Since the variation of the *E*- and *H*-fields in the direction tangential to the boundaries is harmonic with known periodicity, we only need to determine the complex field amplitudes at the interfaces, i.e., we have four unknowns per boundary. The algorithm connects all equivalent sub-problems into a system of $4(N_{layer}-1)$ linear equations with the same number of unknowns (N_{layer} denotes the number of layers). Once the amplitudes of the tangential fields have been determined, it is easy to determine the field amplitudes anywhere in the multilayer structure by applying the homogeneous region equivalent of the layer inside which we want to determine the field value. More details about the G1DMULT algorithm can be found in [4].

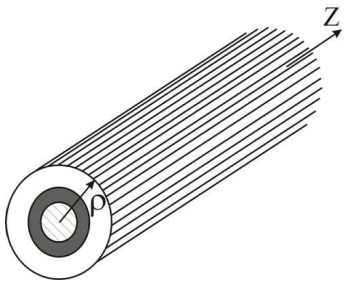

(a) Harmonic one-dimensional problem

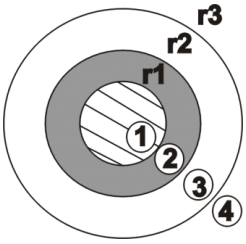

(b) Definition of regions and region boundaries

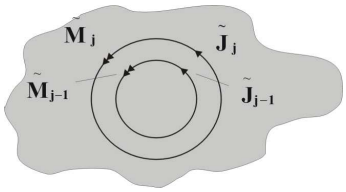

(c) Equivalent problem of region j

Fig. 1. Structure of the G1DMULT algorithm

In order to characterize the considered fiber first we turn our attention to the propagation of surface waves found in cylindrical multilayer structures. Since we are dealing with optical fibers it is important to notice that surface waves correspond to dielectric waveguide modes. They propagate as waves in one-dimensional space, i.e. they do not decay along the fiber axis (if there are no losses in dielectric layers). In the normal direction (ρ direction in our case) they are exponentially decayed in the outermost region. The propagation constant $k_z=\beta_{WM}$ is larger than the wave number of the layer with the lowest refraction index, therefore they are called slow waves. Particular modes will exist only if excited, e.g., if the spectral distribution of the source is nonzero at β_{WM}, and if the source excites some of the field components of the considered optical wave mode. Mathematically, waveguide modes are described by poles of the spectral domain Green's functions, i.e. by the electromagnetic field distribution that can exist without presence of the source (note that the field distribution fulfills the Maxwell equations and boundary conditions).

The poles of the spectral domain Green's function are located between the minimum and maximum wave number, k_{min} and k_{max}, where the wavenumber of the ith region is equal to $k_0 n_i$. For given variation of the surface wave $exp(-jm\phi)$ we can calculate the remaining k_Z integral from (2) as

$$\begin{aligned}&\int_{-\infty}^{\infty}\tilde{G}(k_z,m)e^{-jk_z z}dk_z=\\&=PV\int_{-\infty}^{\infty}\tilde{G}(k_z,m)e^{-jk_z z}dk_z-\sum_k j\pi R_k(m)\end{aligned} \tag{3}$$

Here $\tilde{G}(k_z,m)$ is the Green's function in the spectral domain, PV is the Cauchy's principle value and R_k is the residue of the integrand at the kth pole. Therefore, the function that describes the kth waveguide mode is $-j\pi R_k$. The program first searches for the poles of the spectral domain Green's functions (which correspond to the given ϕ variation of the waveguide mode). The residue is then numerically calculated by multiplying the Green's function with $(k_z-\beta_{WM})$, and evaluating this product at two points near the pole. Since this product is a slowly varying function, the value of the product at the pole is approximated by the mean value of the product at two nearby points.

If the considered fiber has layers with lower refraction index than the one in the core (so-called fiber with depressed inner cladding), it is possible to tailor fiber prop-

erties like the chromatic dispersion characteristic, or to obtain a fiber with low bending losses and splice losses. However, in such fibers the propagating modes can have effective index of refraction lower than the index of refraction of cladding. Therefore, such modes are called leaky modes since the electromagnetic field in the cladding region is not exponentially decaying, i.e. we have a propagating wave in the cladding. The propagation constant and the leakage losses can be estimated if we write the Green's function in the following form

$$\tilde{G}(k_z, m) \cong \frac{\tilde{G}_0(k_z, m)}{k_z - (k_{pole}^{Re} - jk_{pole}^{Im})}, \tag{4}$$

where $\tilde{G}_0(k_z, m)$ is the slowly varying function of k_z, and we can assume that it is constant around the pole. The fact that we have a presence of a leaky wave is explicitly written by approximating the Green's function with the pole that has imaginary part different from zero. This is just an approximation since there is no pole corresponding to the leaky wave mode in the proper Riemann sheet of the function $\sqrt{k_0^2 n_{cladd}^2 - k_z^2}$ (the proper sheet is defined with $\mathrm{Im}\left(\sqrt{k_0^2 n_{cladd}^2 - k_z^2}\right) \leq 0$) [6]. However, there is a pole at the improper Riemann sheet close to the real axis in the k_z-plane, and its presence is the reason why we can approximate the spectral-domain Green's function with (4). This form of spectral-domain Green's functions and the Jordan's lemma [7] enables us to analytically calculate the inverse Fourier transformation (defined with (2))

$$\begin{aligned} I &= \int_{-\infty}^{\infty} \tilde{G}(k_z, m) e^{-jk_z z} dk_z = \\ &= \tilde{G}_0(k_{pole}^{Re}, m) \int_{-\infty}^{\infty} \frac{1}{k_z - (k_{pole}^{Re} - jk_{pole}^{Im})} e^{-jk_z z} dk_z = \\ &= -2\pi j \cdot \tilde{G}_0(k_{pole}^{Re}, m) \cdot e^{-jk_{pole}^{Re} z} e^{-k_{pole}^{Im} z} \end{aligned} \tag{5}$$

The procedure for determining the complex pole is slightly different: the real part of the pole k_{pole}^{Re} is determined by finding the local maximum of the Green's function, and the imaginary part is determined by finding the k_z-points for which the absolute value of the spectral-domain Green's function has 3 dB lower value comparing to the maximum value; for such two points the imaginary part of the pole k_{pole}^{Im} is equal to the difference $k_z - k_{pole}^{Re}$. Note that in the searching procedure only the real form of spectral variable k_z is used.

Once we have determined the propagation constant at the frequency of interest, it is easy to determine other fiber parameters. For example, assuming that only the dominant HE_{11} mode is propagating inside the fiber, the chromatic dispersion coefficient *D* is obtained as

$$D = -\frac{1}{2\pi c} \frac{d}{d\lambda} \left[\lambda^2 \frac{d\beta}{d\lambda} \right], \tag{6}$$

where c is the velocity of light, and the derivatives are calculated using finite difference approach.

2.2 Results

In order to test the developed program first we have compared the results obtained with our program with the results obtained by other analysis methods. The considered fiber has a depressed inner cladding (Fig. 2) and the used parameters are $n_1 = 1.4436$, $n_2 = 1.4364$, $n_3 = 1.4436$, $a_1 = 3.75$ μm and $a_2 = 11.25$ μm. Tables 1 and 2 show the comparison of the calculated propagation coefficient and leakage losses obtained using the present method, the matrix approach [8], [9] and the approximate analytical formula of Cohen *et al.* [10]. As it is evident from Table 1 there is a very good agreement between various methods.

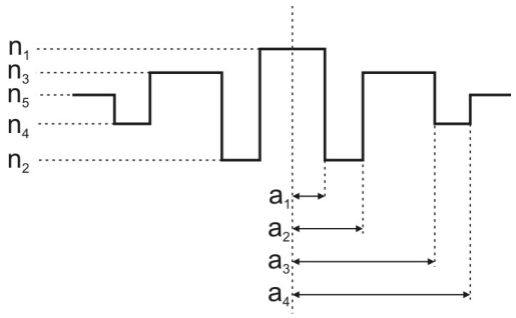

Fig. 2. The refraction index profile of analyzed optical fibers

Table 1. Comparison of the calculated propagation coefficient obtained using different analysis methods

	k_{pole}^{Re}/k_0		
λ (μm)	Present method	[8]	[9]
1.3	1.4405613	1.440568	1.44056849
1.4	1.4402543	1.440262	1.44026234
1.5	1.4399538	1.439963	1.43996259
1.6	1.4396612	1.439671	1.43967071

Table 2. Comparison of the calculated leakage losses obtained using different analysis methods

	Leakage Loss (dB/m)			
λ (μm)	Present method	[8]	[9]	[10]
1.3	36.891	36.87	36.86	37.54
1.4	89.270	88.57	88.51	90.69
1.5	188.61	187.4	186.8	192.4
1.6	357.50	355.8	356.4	366.8

Next we have compared several designs of the multilayer optical fibers by which it is possible to tailor the dispersion characteristics. The values of refractive indices at $\lambda = 1.55\ \mu\text{m}$ and layer radii are given in Table 3; data about double-clad, triple-clad and quadruple-clad fibers are taken from [11], [12] and [13], respectively. The values of n for other frequencies are calculated by interpolating data obtained from the Sellmeier expansion expression corresponding to pure silica and 7.9 mol% GeO_2 doped silica (for layers with index of refraction larger than pure silica) or from the expression corresponding to 1.0 mol% fluorine doped silica (for layers with index of refraction smaller than pure silica); the outermost cladding is made from pure silica [14].

Table 3. Parameters of considered multilayer optical fibers

Single-clad	$n_1 = 1.4495$	$a_1 = 3.8\ \mu\text{m}$
	$n_2 = 1.444$	$a_2 = 125\ \mu\text{m}$
Double-clad	$n_1 = 1.4503$	$a_1 = 3.33\ \mu\text{m}$
	$n_2 = 1.4377$	$a_2 = 4.95\ \mu\text{m}$
	$n_3 = 1.444$	$a_3 = 125\ \mu\text{m}$
Triple-clad	$n_1 = 1.4518$	$a_1 = 3.12\ \mu\text{m}$
	$n_2 = 1.4378$	$a_2 = 4.99\ \mu\text{m}$
	$n_3 = 1.4498$	$a_3 = 6.15\ \mu\text{m}$
	$n_4 = 1.444$	$a_4 = 125\ \mu\text{m}$
Quadruple-clad	$n_1 = 1.4502$	$a_1 = 3.60\ \mu\text{m}$
	$n_2 = 1.4409$	$a_2 = 7.20\ \mu\text{m}$
	$n_3 = 1.4465$	$a_3 = 14.4\ \mu\text{m}$
	$n_4 = 1.4409$	$a_4 = 18.0\ \mu\text{m}$
	$n_5 = 1.444$	$a_5 = 125\ \mu\text{m}$

Fig. 3 shows the field distribution of the basic HE_{11} mode, i.e. the radial dependence of the ϕ-component of the electric field is shown (which is almost equal to the ρ-component). The standard single-clad fiber has larger mode field diameter, but the difference is not too large (see Table 4; the mode field diameter is calculated according to the ITU-T G.650 recommendation). Fig. 4 shows the dispersion characteristics of the considered fibers. Standard single-clad fiber has zero-dispersion around $\lambda = 1.3\ \mu\text{m}$, and the other three have zero-order dispersion around $\lambda = 1.55\ \mu\text{m}$. In [13] it is pointed out that achieving a flat dispersion characteristic for double-clad fibers means that such fibers are usually bend-sensitive for a wide wavelength band. In order to investigate the bending sensitivity we have modified the analysis approach from [15] to calculate bending losses of multilayered fibers. The four considered fibers are compared in Table 4 where we have reported the minimum curvature radius R_{min} ensuring that the pure bending losses are smaller than 0.01 dB/km. It can be seen that the double-clad fiber with flat dispersion characteristic is extremely sensitive to bending; for such applications it is better to use more complex triple-clad or quadruple-clad fibers. We should mention that it is possible to construct a double-clad fiber with low bending losses. However, such a fiber should have much wider depressed inner cladding – the recommended ratio a_2/a_1 is at least three [16], [17].

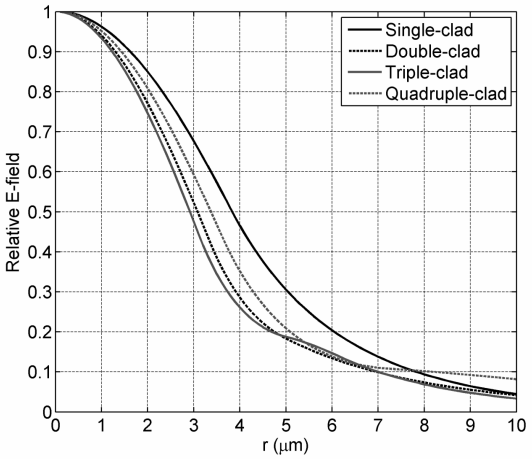

Fig. 3. The HE_{11} mode field distribution at λ_0=1.55 μm. Parameters of the considered fibers are given in Table 2

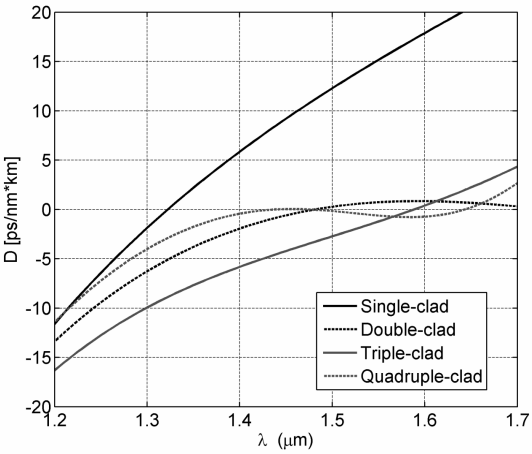

Fig. 4. The chromatic dispersion parameter as a function of wavelength. Parameters of the considered optical fibers are given in Table 2

Besides the possibility of modeling dispersion characteristics in fibers with multiple cladding layers these fibers are also used as active fibers in Ytterbium in-fiber lasers.

Table 4. Mode field diameter and minimum curvature radius at $\lambda = 1.55$ μm of the considered multilayer fibers. The fiber parameters are given in Table 3

	Single-clad	Double-clad	Triple-clad	Quadr.-clad
Mode Field Diameter (MFD) $[\mu\mathrm{m}]$	9.68	7.85	7.62	8.65
Minimum curvature radius $[\mathrm{cm}]$	3.3	8.4	3.7	4.3

Yb fiber lasers are specific because they operate around the wavelength of 1064 nm which is today extensively used for laser cutting. The appropriate operating wavelength, possibility of very high power output, power stability, small spot size are only some of the qualities that these lasers offer. Also, the dissipation of heat that could cause beam distortion is minimized due to the relatively large surface area per unit volume. The analyzed double clad fiber refractive index profile which is considered as a candidate for Yb-laser applications is the one already shown in Fig. 2. The idea behind the depressed inner cladding in this case is to achieve singlemode or near singlemode operation in the core of the fiber. For this analysis the selected parameters were: $n_1 = 1.4625$, $n_2 = 1.4573$, $n_3 = 1.4613$ and $a_1 = 10$ μm. Parameter a_2 was varied in the analysis.

Fig. 5 shows the field distribution of the basic HE_{11} mode and the first higher TE_{01} mode. Here the width of the inner cladding is chosen as a parameter and it shows that the field itself is not greatly affected by the change of the inner cladding width. However, by observing the wavelength dependence of their effective refractive index in Fig. 6 we see that the cutoff wavelength (defined as the wavelength where the effective index becomes equal to the refractive index of the outer cladding) of the TE_{01} mode is lowered as the parameter w is increased and almost reaches the Yb laser design wavelength of 1064 nm. This is significant because it means that with the appropriate selection of parameters the first higher order mode could be pushed into the weakly guiding region, thus leaving only the dominant mode as the guiding one.

The attenuation coefficients for the first two higher order modes are plotted in Fig. 7. For small widths of the depressed layer the attenuation of modes rises rapidly, while with enlarging the width of the depressed layer the rise of the attenuation coefficient is getting slower.

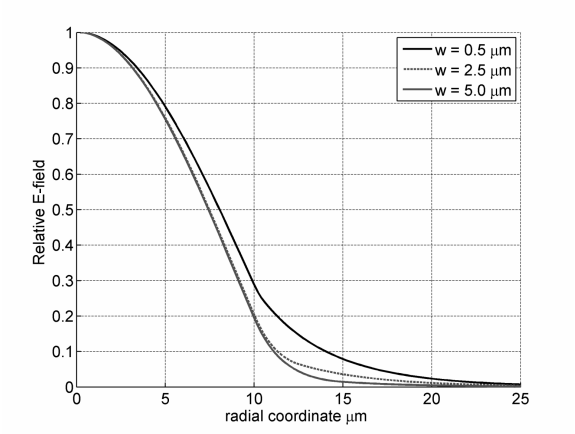

(a) HE_{11} mode

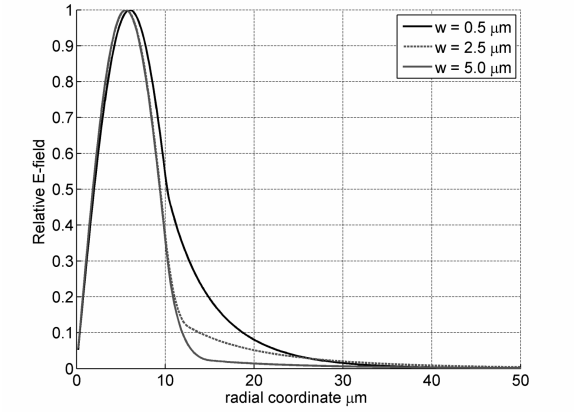

(b) TE_{01} mode

Fig. 5. E-field plot for the HE_{11} and TE_{01} modes with inner cladding width as parameter ($w = a_2 - a_1$)

3 HOLEY FIBERS

3.1 Analysis

Unlike the cylindrically symmetrical layered fibers, photonic crystal fibers generally have a quite different profile. One example of such PCF is the holey fiber (HF) (although holey fibers are not based on photonic crystal properties they are usually regarded as a part of large PCF family of fibers) which has a cladding filled with air holes running down the entire length of the fiber. The transverse index profile of a typical holey fiber with air holes arranged into a periodic triangular lattice, which we will use as an example, is shown in Fig. 8. The darker areas in the figure represent silica and white circles represent the holes.

Since this structure cannot be considered as 1D in the sense described in subsection 2.1, the analysis cannot be performed in spectral domain. Instead the starting point of the analysis will be the modal electric field in spatial

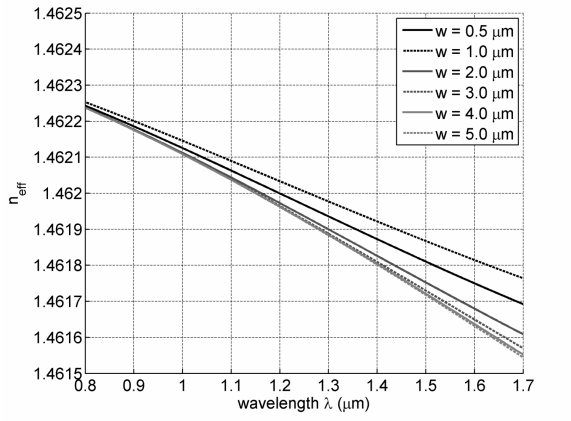

(a) HE_{11} mode

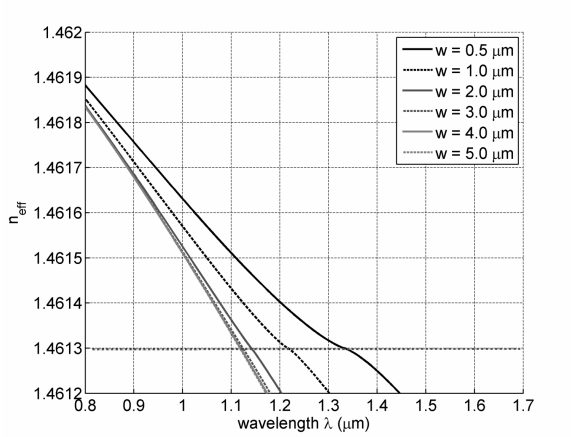

(b) TE_{01} mode

Fig. 6. Cutoff wavelengths for the HE_{11} and TE_{01} modes with inner cladding width as parameter ($w = a_2 - a_1$)

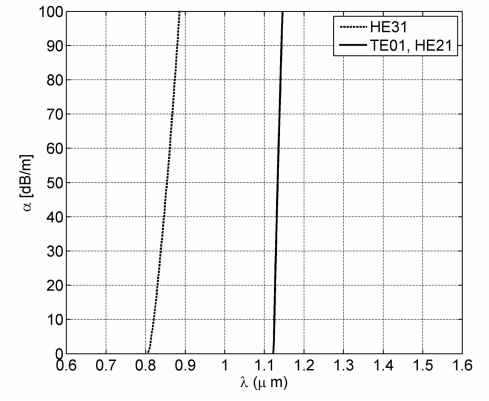

(a) $w = 3.0\ \mu\mathrm{m}$

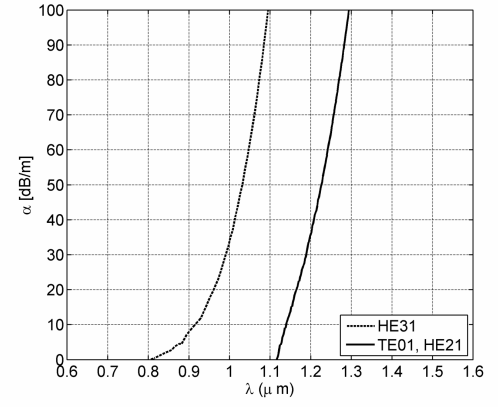

(b) $w = 5\ \mu\mathrm{m}$

Fig. 7. Attenuation of the higher order modes when below cutoff

domain which can be written in the form

$$\vec{E}^i(x,y,z) = \left(e_x^i(x,y)\hat{x} + e_y^i(x,y)\hat{y} + e_z^i(x,y)\hat{z}\right) e^{j\beta_i z}, \tag{7}$$

where β_i is the propagation constant of the ith mode and e_x, e_y and e_z are the electric field components. We naturally assume that the fiber is uniform in the axial (z) direction. Inserting this formulation into the vector wave equation we obtain a pair of coupled equations for the e_x and e_y field components in a source free fiber [18]:

$$\begin{aligned}\left\{\nabla^2 + n^2k^2 - \beta^2\right\} e_x &= -\frac{\partial}{\partial x}\left(e_x\frac{\partial \ln(n^2)}{\partial x} + e_y\frac{\partial \ln(n^2)}{\partial y}\right)\\ \left\{\nabla^2 + n^2k^2 - \beta^2\right\} e_y &= -\frac{\partial}{\partial y}\left(e_x\frac{\partial \ln(n^2)}{\partial x} + e_y\frac{\partial \ln(n^2)}{\partial y}\right)\end{aligned} \tag{8}$$

where k is the wavenumber and $n = n(x,y)$ is the transverse refractive index profile.

These equations are solved by decomposing the electric field into a series of orthogonal functions described with

$$e_x(x,y) = \sum_{a,b=0}^{N} \left(w_{ab}\xi_a(x)\xi_b(y)\right), \tag{9}$$

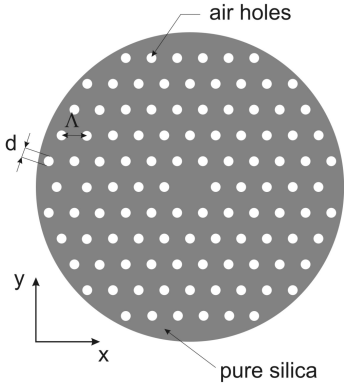

Fig. 8. Transverse index profile of a holey fiber

where ξ_a are the chosen basis functions and w_{ab} are the required weighting coefficients. Good results can be obtained using Hermite-Gaussian [19] or cosine orthonormal basis functions [20]. Naturally, the e_y field component is described in the same manner.

Implementing the decomposition of the electric field modes (9) into the equations for the modal electric fields (8) gives us a single equation with $N \times N$ unknowns, which then needs to be expanded to a full set of $N \times N$ equations using the same set of Hermite-Gaussian or cosine orthogonal functions. These equations are then integrated over the (x, y)-plane in order to obtain the following eigenvalue equations:

$$\begin{aligned} M_x \hat{v}_x &= \tfrac{\beta_x^2}{k^2} \hat{v}_x, \\ M_y \hat{v}_y &= \tfrac{\beta_y^2}{k^2} \hat{v}_y, \end{aligned} \tag{10}$$

where $\hat{v}_{x,y}$ are eigenvectors defined with the field weight coefficients, and M is the system matrix which contains the resulting overlapping integrals. It needs to be pointed out that the resulting eigenvalue equations are obtained with the assumption that our holey fiber is symmetric. With this assumption the fundamental modes can be considered linearly polarized and consequently this leads to decoupling of the equations for e_x and e_y in (8).

3.2 Results

The results obtained using the presented analysis were compared to the measurements done on a test holey fiber LMA-15 whose microscope image is shown in Fig. 9 (LMA-15 fiber is provided by Crystal Fibre A/S). The ratio of the hole diameter and the spacing between the holes for this fiber is approximately $d/\Lambda = 0.45$ which allows it to work as in singlemode operation in a very wide range of wavelengths (500 – 2000 nm).

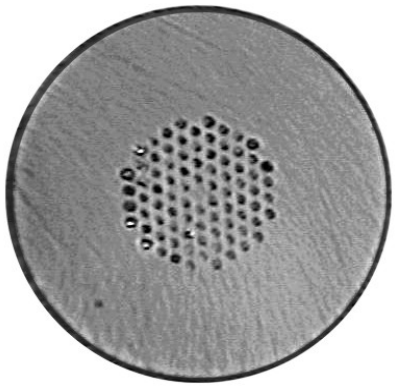

Fig. 9. Microscope image of LMA-15 fiber end

This so-called endlessly singlemode operation can be intuitively explained using the effective refractive index of the cladding and the expression for the normalized fiber frequency V

$$V = \frac{2\pi\rho_{core}}{\lambda}\sqrt{n_{core}^2 - n_{clad,eff}^2}. \tag{11}$$

Unlike the fibers with a homogeneous cladding where the difference between the refractive indices of the core and the cladding is constant, in the holey fiber case this difference is reduced when the wavelength goes down. Consequently from (11) we see that this reducing difference actually compensates for the reducing wavelength and keeps the normalized frequency below the singlemode threshold at $V = 2.405$. This happens because the field at lower wavelengths is more tightly confined to higher refractive index regions (silica), thus raising the effective refractive index of the cladding. As the effective cladding index is increased, its difference with the respect to the core is reduced. Thanks to this particular property of the LMA-15 fiber it was possible to use 650 nm laser for the measurements.

The recorded image of the output intensity from the tested fiber is shown in Fig. 10a and it clearly shows that only one mode is present in the output field. For comparison the output from a standard G.652 fiber at 650 nm is given in Fig. 10b which is as expected multimode at this wavelength. The computed output intensity for the considered holey fiber is given in Fig. 11 and although it was not possible to obtain the exact values of the field intensity in the measured result, there is an obvious visual match with the calculated intensity. Also the calculated result showed a strong confinement of the field to the core region as expected at the considered wavelength.

An additional benefit which holey fibers have is their insensitivity to bending. This insensitivity is a consequence of the air holes. Namely, the effective refractive index is lowered as we move away from the solid silica core into the holey region and consequently the light in these regions can travel faster. Thus, even in the case of severe bending the wave front of the particular mode will be maintained and no losses will occur.

In order to verify this property, the test LMA – 15 fiber was submitted to a series of bend loss measurements. Bending radii which were considered were 15 mm and 5 mm and in both cases 10 turns were made. These measurements were compared to the measurements of standard G.652 fiber done under the same conditions. Fig. 12 shows the comparisons between the results obtained for the G.652 and the LMA – 15 fibers for two different bending radii. It is clear in both cases that the LMA – 15 fiber has significantly lower bending losses compared to the standard fiber.

4 CONCLUSION

This paper discusses analysis approaches for novel types of optical fibers with different alternative cladding

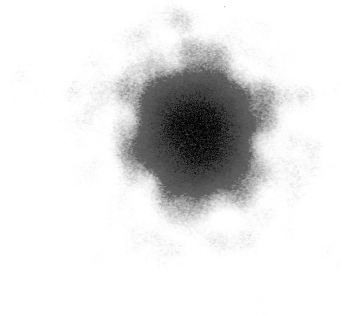

(a) For LMA-15 fiber

(b) For G.652 standard fiber

Fig. 10. Recorded images of field intensities at 650 nm

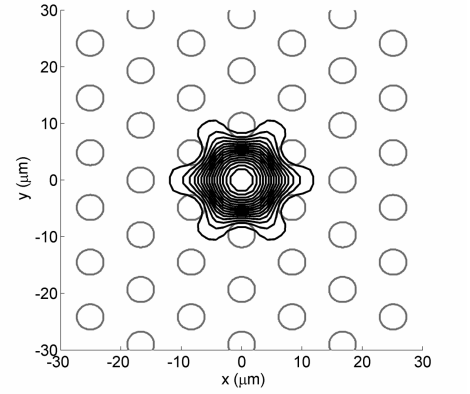

Fig. 11. Calculated intensity plot for the LMA – 15 fiber using 7 Hermite – Gaussian modes

geometries. In the primary focus are optical fibers with multilayered claddings which are being reinvented due to the possibility to tailor their properties for various new custom applications. Since the only variation in the cladding structure is in the radial direction it was possible to ap-

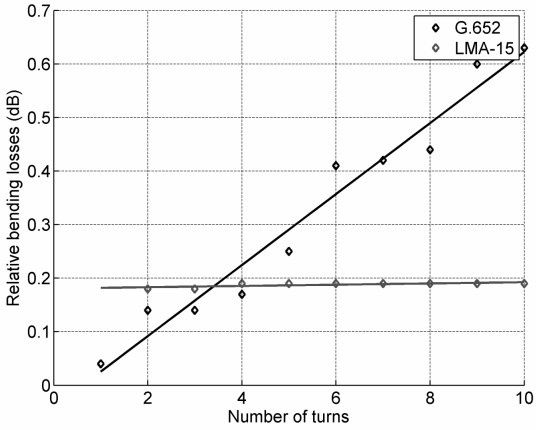

(a) Bending radius is 15 mm

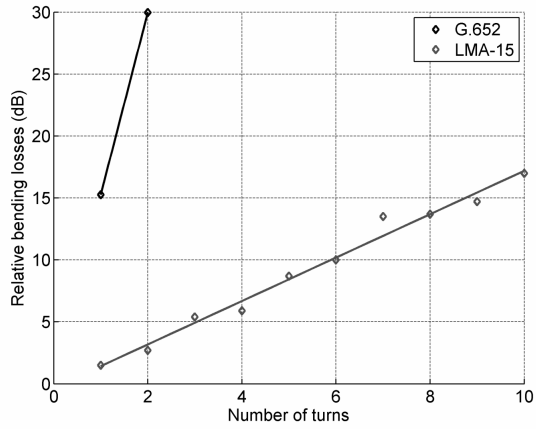

(b) Bending radius is 5 mm

Fig. 12. Measurements of bending losses for standard G.652 fiber and LMA – 15 fiber

ply spectral domain analysis approach, i.e. to calculate the corresponding Green's functions in the spectral domain. This was done using a numerical G1DMULT algorithm which allows the analysis of multilayered structures with arbitrary number of layers in the cladding. From the obtained Green's functions it is possible to characterize the considered fiber by analyzing the poles of the Green's functions since the poles correspond to the actual optical fiber modes. Furthermore, by analyzing the behavior of the propagation constant of the considered mode, the information regarding attenuation and dispersion properties can be found. Although these fiber types could be analyzed even strictly analytically, the advantage of this approach lies in the fact that fibers with practically any number of cladding layers can be analyzed. Also, unlike the analytical case where a change in the analyzed structure requires a new derivation, here every change can be easily adopted. Nu-

merical results of this approach were presented for various cladding geometries and found to be in good agreement with test cases found in literature.

The second part of the paper deals with the analysis of holey fibers which belong to the group of so-called Photonic Crystal Fibers. Holey fibers have a cladding filled with a periodic lattice of small air holes. Although these air holes extend throughout the entire length of the fiber, thus making the structure even symmetrical around the central axis, it was not possible to apply spectral domain approach in this case. For that reason the analysis is based on solving the vector wave equation by expanding the electric field into cosine or Hermite-Gaussian modes. Using this approach a commercial fiber was analyzed and the results showed good agreement with the measured ones.

REFERENCES

[1] A. Mendez and T.F. Morse, **Specialty optical fibers handbook**, Academic Press, 2007.

[2] G. Keiser, **Optical fiber communications**, McGraw-Hill, 1999.

[3] P.L. Daniels, **Analytical expression for group delay in the far field from an optical fiber having an arbitrary index profile**, IEEE J. Quantum Electron., vol. QE-17, pp. 850–853, 1981.

[4] Z. Šipuš, P.-S. Kildal, R. Leijon, and M. Johansson, **An algorithm for calculating spectral domain Green's functions for planar, circular cylindrical and spherical multilayer structures**, Applied Computational Electromagnetic Society Journal, vol. 13, pp. 243–254, 1998.

[5] C. Balanis, **Advanced Engineering Electromagnetics**, Wiley, 1989.

[6] W.C. Chew, **Waves and Fields in Inhomogeneous Media**, IEEE Press, 1995.

[7] S. Kurepa and H. Kraljević, **Funkcija kompleksne varijable**, Tehnička knjiga, Zagreb, 1986.

[8] M. R. Shenoy, K. Thyagarajan, and A. K. Ghatak, **Numerical analysis of optical fibers using matrix approach**, IEEE J.Lightwave Technol., vol. 10, pp. 1285–1290, 1988.

[9] K. Thyagarajan, Supriya Diggavi, Anju Taneja, and A. K. Ghatak, **Simple numerical technique for the analysis of cylindrically symmetric refractive-index profile optical fibers**, Applied Optics, vol. 30, pp. 3877–3879, 1991.

[10] L. G. Cohen, D. Marcuse, and W. L. Mammel, **Radiating leaky mode losses in single mode lightguides with depressed index claddings**, IEEE J. Quantum Electron., vol. 18, pp. 1467–1472, 1982.

[11] M. Monerie, **Propagation in Doubly Clad Single-Mode Fibers**, IEEE Journal of Quantum Electronics, vol. QE-18, pp. 535–542, 1982.

[12] Y.W. Li, C.D. Hussey, and T.A. Birks, **Triple-Clad Single-Mode Fibers for Dispersion Shifting**, IEEE Journal of Lightwave Technology, vol. LT-11, pp. 1812–1818, 1993.

[13] P.L. Francois, **Propagation mechanisms in quadruple-clad fibres: mode coupling, dispersion and pure bend losses**, Electronics Letters, vol. 19, pp. 885–886, 1983.

[14] M. J. Adams, **An introduction to optical waveguides**, Chichester: Wiley, 1981.

[15] D. Marcuse, **Curvature loss formula for optical fibers**, J. Opt. Soc. Amer., vol. 66, pp. 216–220, 1976.

[16] J. Auge, C. Brehm, L. Jeunhomme and C. le Sergent, **Parametric study of depressed inner cladding single-mode fibers**, IEEE Journal of Lightwave Technology, vol. LT-3, pp. 767–771, 1985.

[17] K. Himeno, S. Matsuo, N. Guan and A. Wada, **Low-bending-loss single-mode fibers for Fiber-to-the-Home**, IEEE Journal of Lightwave Technology, vol. LT-23, pp. 3494–3499, 2005.

[18] A. W. Snyder and J. D. Love, **Optical Waveguide Theory**, Chapman and Hall Ltd, 1983.

[19] T. M. Monro, D. J. Richardson, N. G. R. Broderick, P. J. Bennett, **Modeling Large Air Fraction Holey Optical Fibers**, Journal of Lightwave Technology, vol. 18, pp. 50–56, 2000.

[20] M. Bosiljevac, **Modeling of Photonic Crystal Fibers**, in Proceedings of the 19th International Conference on Applied Electromagnetics and Communications, Dubrovnik, 2007, pp. 313–316.

Zvonimir Šipuš was born in Zagreb, Croatia, in 1964. He received the B.Sc. and M.Sc. degrees in electrical engineering from the University of Zagreb, Croatia, in 1988 and 1991, respectively, and the Ph.D. degree in electrical engineering from Chalmers University of Technology, Gothenburg, Sweden, in 1997.
From 1988 to 1994, he worked at Ruđer Bošković Institute, Zagreb, Croatia, as Research Assistant, involved in the development of detectors for explosive gases. In 1994, he joined the Antenna Group at Chalmers University of Technology, where he was involved in research projects concerning conformal antennas and soft and hard surfaces. In 1997 he joined the Faculty of Electrical Engineering and Computing, University of Zagreb, where he is now a Professor. Since 2008 he is the Head of the Department of Wireless Communications there. From 1999-2005 he was also an adjunct researcher at the Department of Electromagnetics, Chalmers University of Technology. His main research interests include numerical electromagnetics with application to antennas, microwaves, and optical communications.

Marko Bosiljevac was born in Zagreb, Croatia, in 1980. He received his B.Sc. degree from the Faculty of Electrical Engineering and Computing, University of Zagreb in 2005. Currently he is a research assistant at the Department of Wireless Communications of the Faculty of Electrical Engineering and Computing, University of Zagreb. His research interests include advanced numerical techniques and acceleration methods for applications in antennas, microwaves and optics.

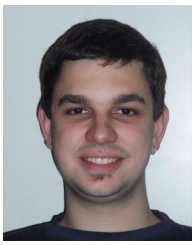

Ivan Lujo was born in Dubrovnik, Croatia, in 1984. He graduated from the University of Zagreb, Faculty of Electrical Engineering and Computing in 2007. His research interests are propagation in optical fibers and fiber based sensor systems. He is currently employed as an assistant on the Polytechnic of Zagreb, Dept. of Electrotechnics.

AUTHORS' ADDRESSES

Prof. Zvonimir Šipuš, Ph.D.
Marko Bosiljevac, M.Sc.
Department of Radiocommunications and Microwave Engineering,
Faculty of Electrical Engineering and Computing,
University of Zagreb,
Unska 3, HR-10000 Zagreb, Croatia
emails: zvonimir.sipus@fer.hr,
marko.bosiljevac@fer.hr

Ivan Lujo, M.Sc.
Department of Electrotechnics,
Polytechnics of Zagreb,
Vrbik 8, HR-10000 Zagreb, Croatia,
email: ivan.lujo@tvz.hr

Received: 2009-11-02
Accepted: 2009-11-27